

POWER SYSTEM SECURITY OF THE POWER FLOW COMPUTATION ON DISTRIBUTION ELECTRIC NETWORK USING RENEWABLE ENERGY SOURCES

Constantin GHINEA¹, Mircea EREMIA², Lucian TOMA³

This paper presents power flow calculation for a distribution electric network, based on known recordings of the energy meters such as the average hourly active and reactive powers of consumers and the power injections from renewable energy sources for one year. A research is carried out on the operation of the electric network and on the influence that the connection of two renewable sources has on lines loading, voltage magnitude and active power losses.

Keywords: power flow, renewable energy sources (RES)

1. Introduction

The fast development of renewable energy sources raises challenges and opportunities regarding their integration into electric networks [1].

Given the fact that the wind and solar energy have the biggest growth out of the renewable sources, many studies have been performed on the impact of voltage stability, power losses or the effects of harmonic distortion [2], [3], [4].

The most effective tool for evaluating the behavior of power system operation process is the computation of the power flow. This is a mandatory step, both of the operative planning and operation as well as in the case of design studies and development of electric transmission and distribution networks. In a review of existing research and available literature, there are studies that analyze the impact of distributed sources on electric networks, as well as the use of methods for optimal location of RES [5], [6], [7].

Use of direct methods, in the case of large - scale electric networks, conduct to long computation times and are uneconomical in terms of used memory. Seidel - Gauss methods require a large number of iterations and can raise convergence issues. In this context, for the power flow calculation of the electric networks, the Newton - Raphson method became widely spread, which ensures better convergence, in a small number of iterations [8], [9].

¹ PhD student, Department of Electrical Power Systems, University POLITEHNICA of Bucharest, Romania, e-mail: costi.ghinea@yahoo.com

² Prof. Em., Department of Electrical Power Systems, University POLITEHNICA of Bucharest, Romania, Romania, e-mail: eremia1@yahoo.com

³ Assoc. Prof., Department of Electrical Power Systems, University POLITEHNICA of Bucharest, Romania, Romania, e-mail: lucian.toma@upb.ro

With the new update of energy policy framework, called the "Clean energy for all Europeans package", European Union adopted new ambitious targets, such as: a share with at least 32% for renewable energy sources in the EU's energy mix by 2030, at least 32,5% energy efficiency by 2030 and at least 40% cuts in greenhouse gas emissions (from 1990 levels) [10]. Consequently, the increasing penetration of RES will lead to new challenges regarding the design, the development and the operation of electricity networks.

2. Power flow algorithm using Newton - Rapshon method

The power flow computation of the electric networks aims at the full determination of the main elements associated with the nodes and branches.

Fig. 1 illustrates the flow chart explaining the power flow algorithm used to perform this calculation.

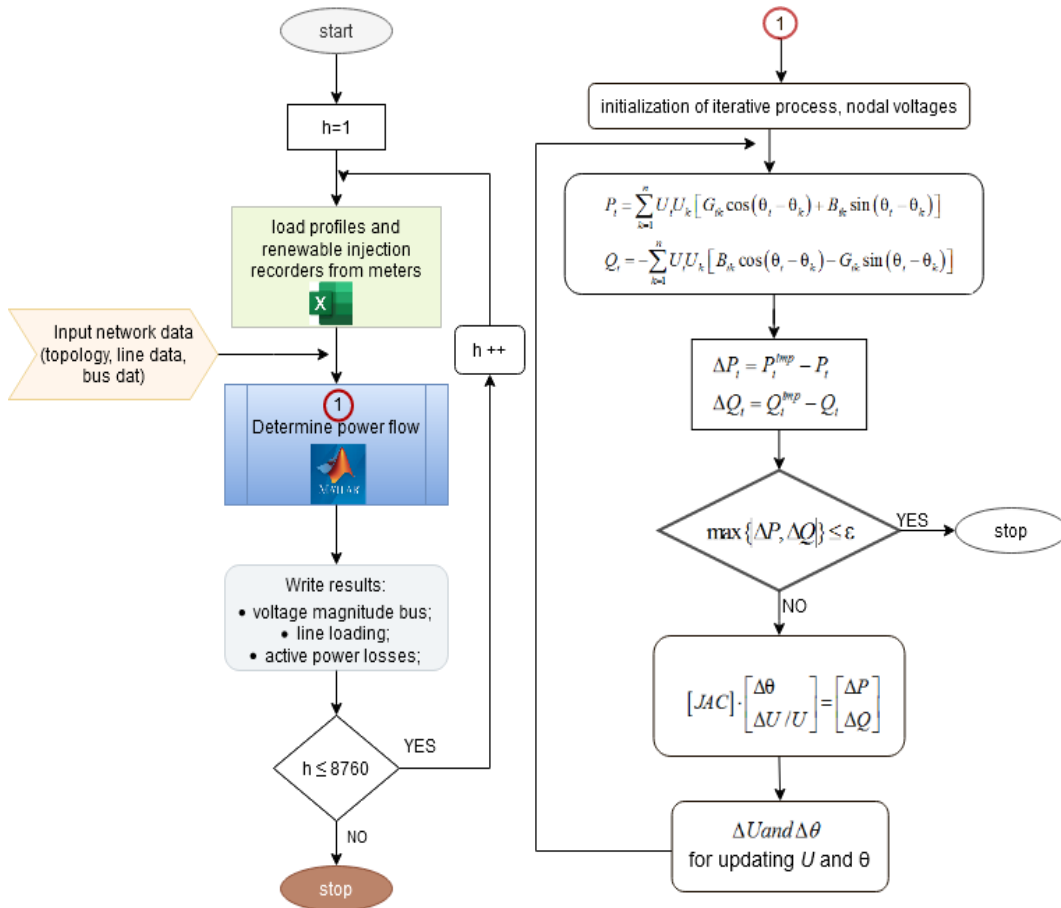


Fig. 1. Flow chart of the algorithm

In the basic formulation of the load flow study, four variables are associated to each node: active power P , reactive power Q , the voltage magnitude U and phase-angle θ (calculated in relation to an arbitrarily selected axis of reference), grouped in two complex expressions $\underline{S} = P + jQ$ and $\underline{U} = Ue^{j\theta}$ [11].

The Newton - Rapshon method can be applied to solve any set of nonlinear equations of the form. The convergence of the Newton method is essentially conditioned by the first approximation of the solution, which is necessary to be close enough to the exact solution. The algorithm continues with the determination of a new correction and approximation until they become sufficiently small [12]. If the node in question, in addition to the generated powers (P_g^{RES}, Q_g^{RES}) is consumed P_c or Q_c , the complex apparent power of the node become: $\underline{S} = P_c + jQ_c - (P_g^{RES} + jQ_g^{RES})$.

3. Case study and results

In the case study, the average hourly active and reactive powers are known for different types of consumers, based on energy meter records, for one year. The 20 kV medium voltage distribution electric network, that ensure supply to the ten consumers via eleven underground cables, is shown in Fig. 2. The load and the generation profiles are real, eventually scaled up or down. The network configuration is not real; it is intended to be of appropriate size that allows an easily analyze of the results. However, the line parameters, $r=0,16 [\Omega/km]$ and $x=0,1 [\Omega/km]$ correspond to real cables and the distribution network Test - 20 kV is specific to a suburban area.

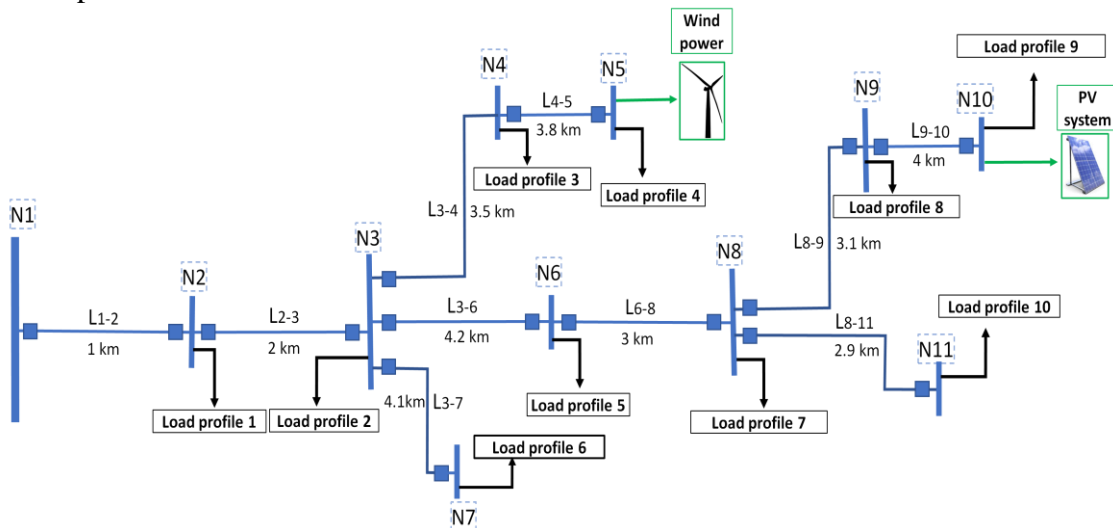
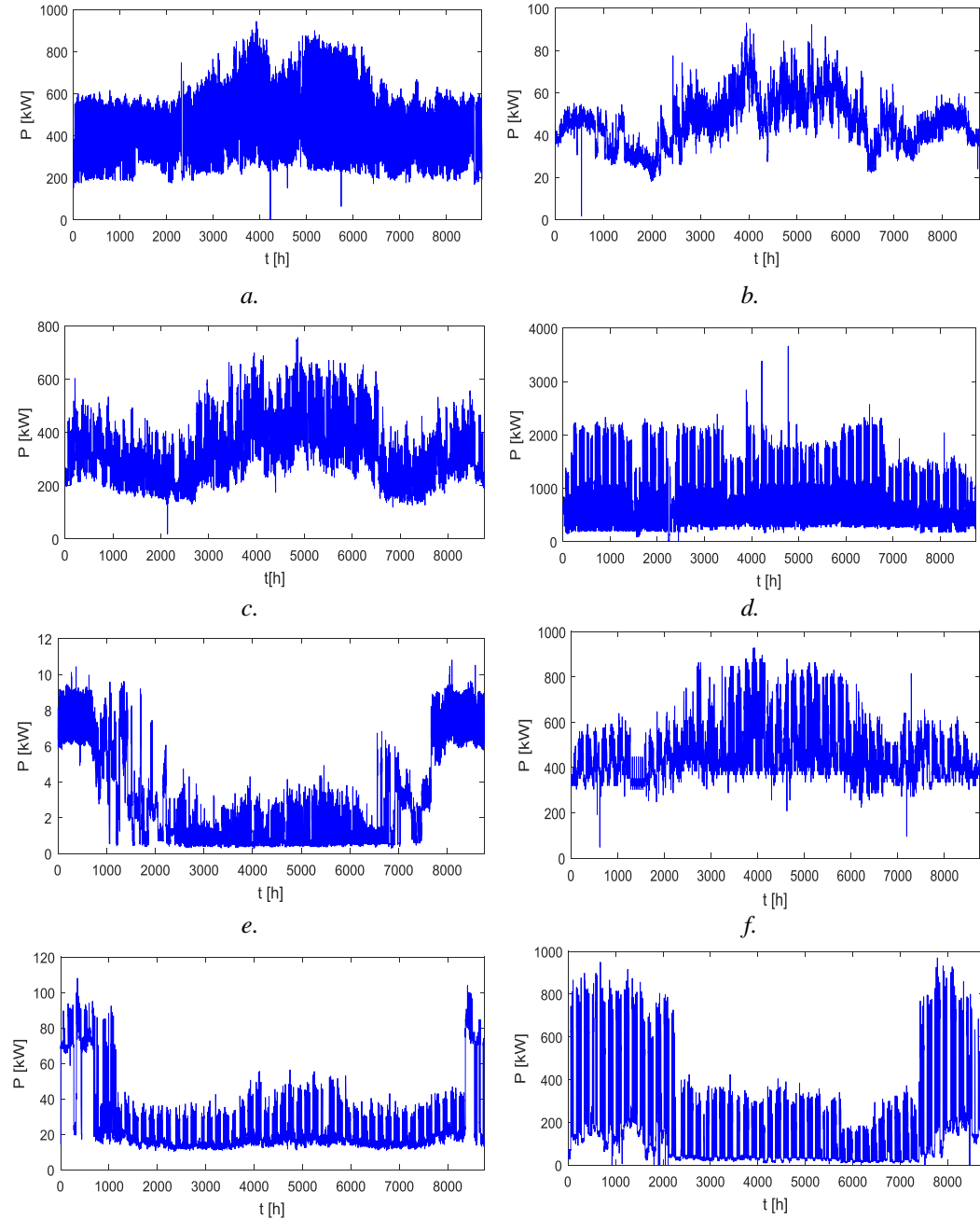


Fig. 2. Distribution network Test - 20 kV.

In Fig. 3, load profiles are shown. They illustrate the active power variation, or different types of consumers, such us: supermarket - load profile 1, subway - load profile 4, hospital - load profile 10, industrial consumer - load profile 9, pharmacy - load profile 5 and five different commercial consumers for the other load profiles.



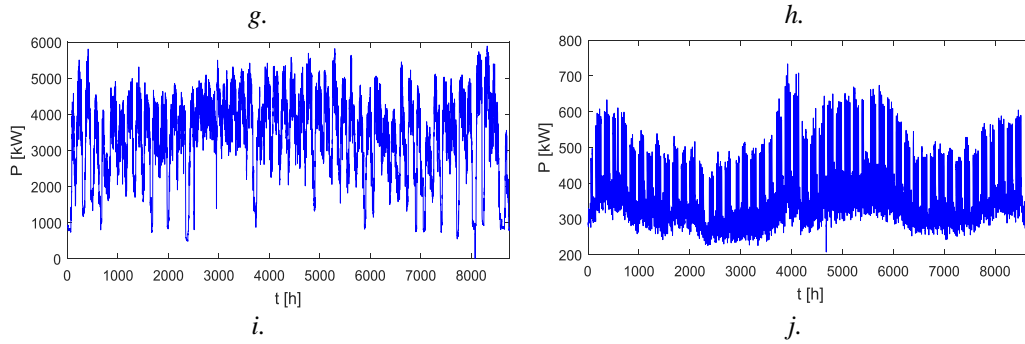


Fig. 3. Active power measured for one year:
a. Load profile 1; *b.* Load profile 2; *c.* Load profile 3; *d.* Load profile 4;
e. Load profile 5; *f.* Load profile 6; *g.* Load profile 7; *h.* Load profile 8;
i. Load profile 9; *j.* Load profile 10.

Further, it was analyzed the influence on active power losses, the limitations in terms of voltage magnitude and network loading, when two renewable energy sources are connected. The wind power ($P_{wind}=1000\text{ kW}$) and the PV system ($P_{solar}=2877,8\text{ kW}$) are connected to bus 5 and 10. The generation curves based on the average hourly active power injected in one year are shown in Fig. 4.

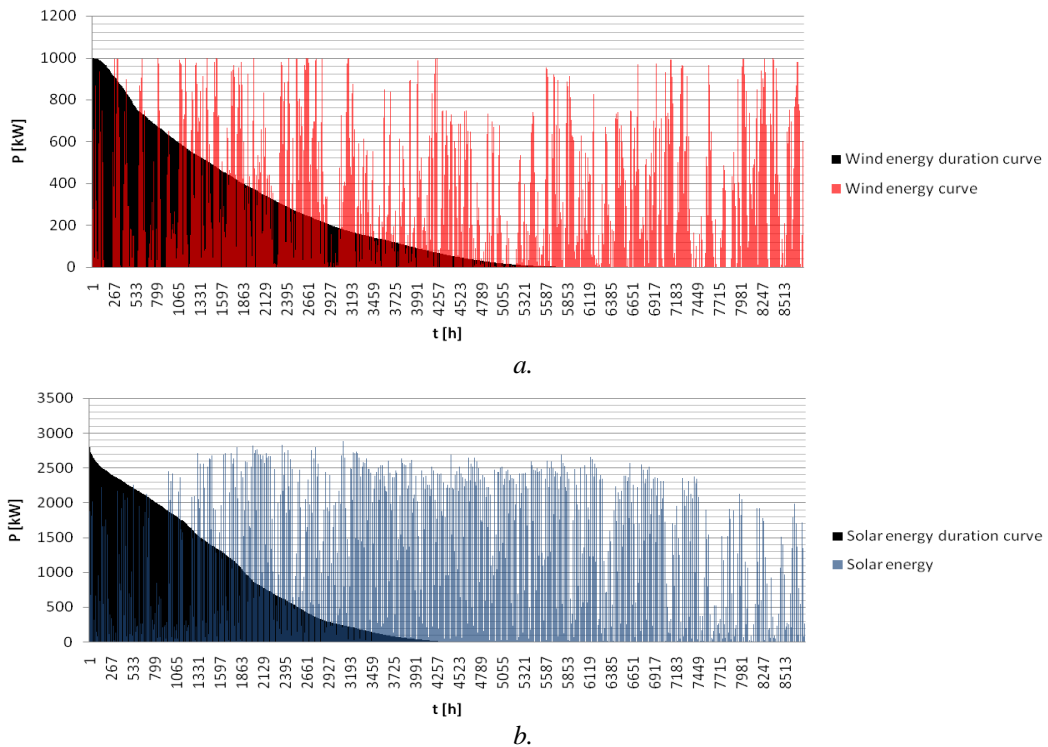


Fig. 4. Generation curve: *a.* Wind system; *b.* PV system.

RES generate active power in about 68% for wind system and 50% for solar system, considering the analyzed time (one year). There is also no power injection from both renewable energy sources in 1443 hours.

Table 1 indicates the percentage probabilities for which there is an increase of the voltage magnitude at PQ nodes due to the connection of the renewable energy sources.

Table 1.

Probabilities values for magnitude voltage increases

Probability [%] Month:	Bus 2	Bus 3	Bus 4	Bus 5	Bus 6	Bus 7	Bus 8	Bus 9	Bus 10	Bus 11	Average
January	24,3	46,4	54,6	58,5	49,7	46,2	51,1	51,1	53,6	51,5	48,7
February	30,7	55,2	63,8	67,3	60	54,6	61,2	63,2	63,4	59,8	57,92
March	40,6	65,7	74,2	78,5	66,4	64,1	66,4	67,5	69	66,3	65,87
April	46,1	67,9	76	77,4	72,8	69,9	73,5	73,8	74,6	72,9	70,49
May	42,3	59,7	69	71,2	64,7	61	66,1	66,9	66,5	65,9	63,33
June	47,6	64	68,8	73,5	69,3	66	71	71,3	72,6	70,3	67,44
July	47,6	64,1	68,2	68,6	66,9	63,7	68,8	68,6	69,8	68,4	65,47
August	44,1	57,9	61,4	61,6	60,9	58,1	62,9	64,5	63,7	62	59,71
September	38,2	57,5	63,1	65,1	59	56,9	59,7	60,6	61,4	60,7	58,22
October	38,7	60,1	68,4	70,3	63,2	60,5	64,9	63,3	63,8	63,3	61,65
November	22,4	41	47,2	52,8	45,1	41,4	48,6	47,2	47,6	46,1	43,94
December	25,3	56,2	65,7	70,8	57	57,4	59,3	58,2	59,3	59,5	56,87

The table values are realized by computing the percentage of increases in the voltage magnitude in a month period, taking in account the total number of hours, for every bus, after the connection of RES. A color scale is applied to table 1 so that the highest increases are colored in green, the medium in orange, and the lowest value are colored in red.

When we take in consideration all the 8760 hours analyzed, at bus 5 and 10, there is produced an average voltage magnitude augmentation that reached the value of 67,97% and 63,78%, respectively. Also, in April, June and July, the highest percentage of increases of the parameters is registered, due to the important injection of PV (long day's solar irradiation) and wind systems. Therefore, by connecting the renewable energy sources, for bus 4, 5, 8, 9, and 10, a significant improvement of the voltage level is observed. A comparison for bus 10 and 5 in July is illustrated in Fig. 5.

For the entire study period, connecting the PV to bus 10 leads to a higher voltage increase rather than the wind source at bus 5, whose input on the voltage magnitude is lower due to the difference of installed power on one hand and load bus consumption on another hand.

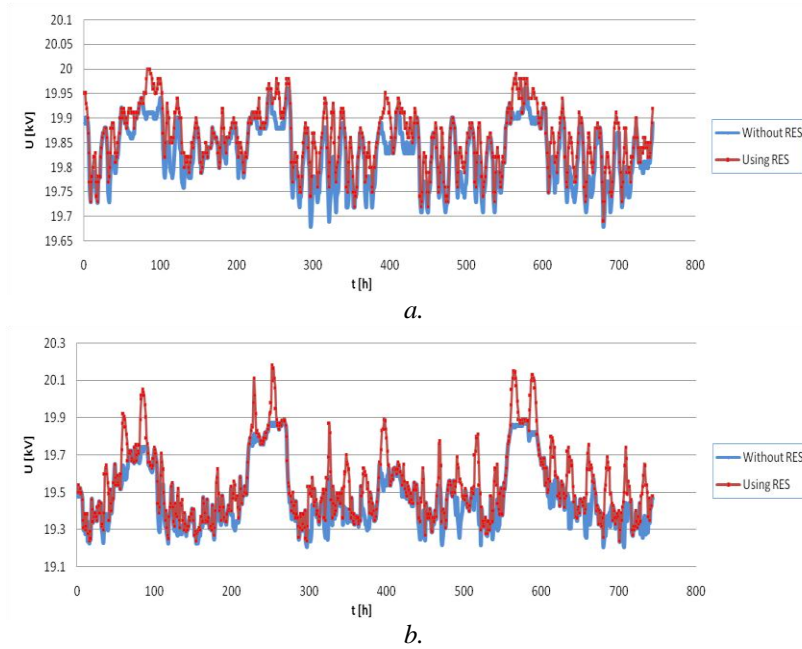


Fig. 5. Voltage variation for July: a. Bus 5; b. Bus 10.

The calculated periods for the line loading L_{1-2} are represented in Fig. 6. Connecting RES had lead to a decrease with a period of 585 (793-208) hours for the overloading with more than 70%. Also, analyzing all the intervals below, the overloading range with the most significant decrease in value, after the renewable energy sources connection, is recorded in the area $[60 \div 70]$, the gain being 805 (1911-1106) hours. The trend of values drawn with dotted lines is realized by inserting the moving average. It is used to analyze the continuity of the resulting data and to obtain general information about the progress direction.

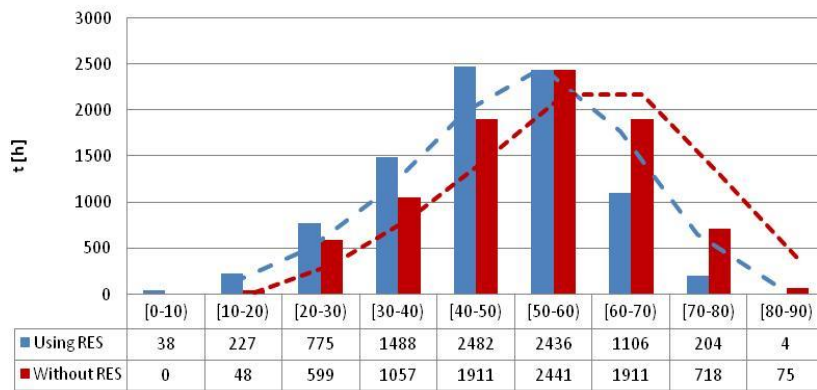


Fig. 6. Line loading L_{1-2}

Table 2

Loading elements results summarized considering maximum production from RES

<div>Element:</div> <div>Lines loading [%]</div>		L_{1-2}	L_{2-3}	L_{3-6}	L_{6-8}	L_{8-9}	L_{9-10}
January	using RES	28,1	23,8	19,8	20	16,4	10,9
	without RES	52,3	47,9	35,9	36	32,2	25,9
February	using RES	13,6	9,5	1,9	2,4	3,6	5,3
	without RES	39,9	35,7	22,9	22,9	18,5	17,2
March	using RES	28,8	25,2	18	18,5	15,5	13,9
	without RES	58,6	54,8	39,6	39,9	36,1	33,4
April	using RES	8,6	12,8	16,4	16,2	18,3	18,5
	without RES	22,4	18,3	7,4	7	4,4	4
May	using RES	35,7	31	18,8	19,5	17,2	17,5
	without RES	62,7	57,9	38,1	38,4	35,2	35
June	using RES	36,1	28,5	15,9	16,5	14,3	14,8
	without RES	61,3	53,8	36	36,2	33,1	33,2
July	using RES	49	43,1	27	27,5	23,4	22,9
	without RES	76,5	70,7	48,5	48,8	44,1	43,1
August	using RES	45,2	38,7	23,3	23,8	19,3	18,6
	without RES	73,8	67,3	44,2	44,5	39,1	37,8
September	using RES	34,7	30,2	17,6	18,2	15,6	15,4
	without RES	58,5	53,9	35,4	35,7	32,3	31,9
October	using RES	25,4	21,1	14,9	15,4	12,8	12,3
	without RES	51,6	47,2	33,5	33,7	30,2	28,9
November	using RES	11,2	7,4	7	6,7	10,8	13,1
	without RES	30	25,9	12,6	12,5	8,2	6
December	using RES	17,2	13,2	3,6	3	1,6	6,8
	without RES	36,4	32,3	17,5	17,3	12,8	7,5

Table 2 shows a decreasing of loading elements for the case of maximum injected power from wind and PV system in the network Test - 20 kV. The values were achieved after detecting the interval (one hour), for each month, when maximum injection from renewable energy sources is considered. The values run between 2935,65 kW in January to a maximum of 3713 kW in April. For L_{1-2} , it is noted that when RES injected maximum power, the loading level decreased by approximately 65,91 % in February and by 50,85 % in March.

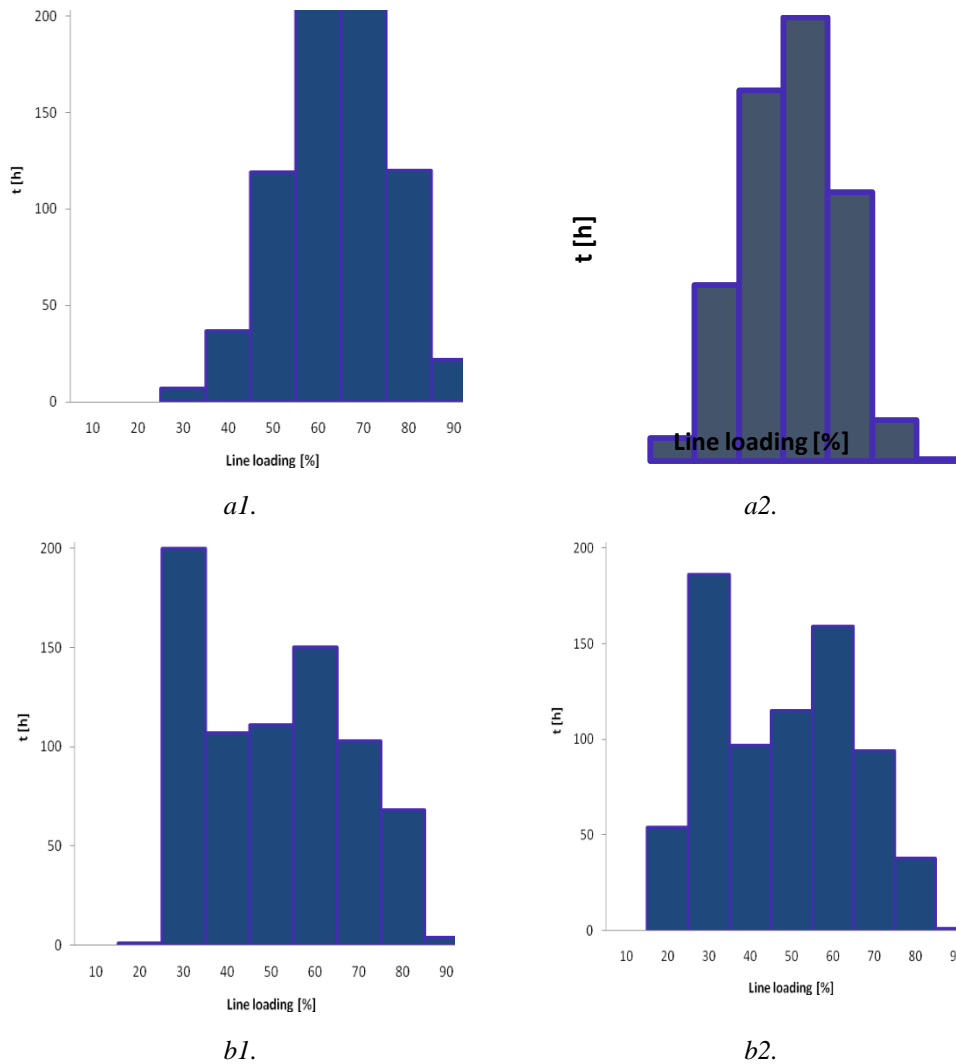


Fig. 7. Line loading analysis for:
a1. July without RES; *a2.* July using RES;
b1. December without RES; *b2.* December using RES.

Fig. 7 is illustrated the line loading hour frequency for L_{1-2} considering the case without / using RES. The time periods analyzed in July and December are the most representative due to the demand of nodes consumers. Connecting the renewable energy sources leads to a decrease of overloading hours. Also, it can be observed that the trend of values is orientated to the average ones, with significant decrease for time periods values in the interval $(60\div90)\%$.

Fig. 8 presents the annual average active power losses for the elements of network Test - 20 kV. From the analysis of the results, by connecting wind system and PV system, for L_{1-2} and L_{2-3} , there is a reduction of active power losses that reached 19,6 % and 20,6 % respectively. Also, when wind system injects power at bus 5, active power losses for L_{4-5} are reduced by 22,3 %.

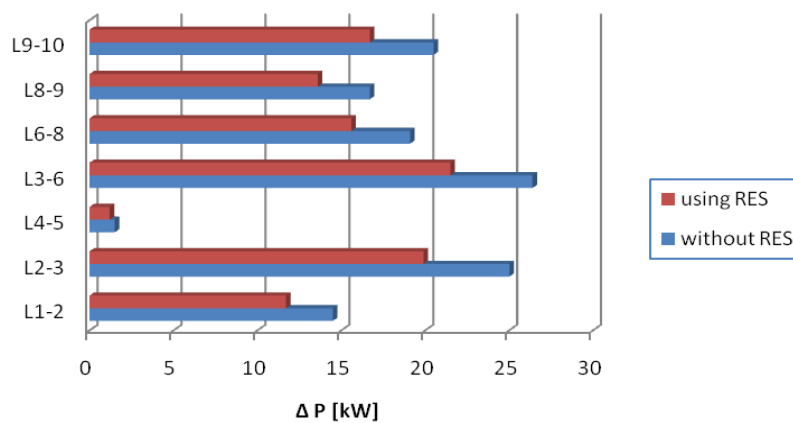


Fig. 8. Active power losses for underground cables.

In order to observe the impact of renewable energy sources, a graphic illustrated the average active power losses during one month are depicted in Fig. 9. After the renewable energy sources connection, the values decreased and their trend can be observed using the red color area.

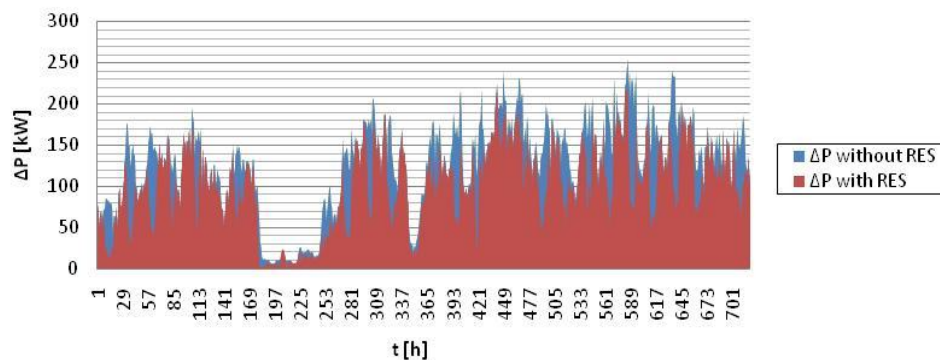


Fig. 9. Average active power losses for April

In Fig. 10, in order to minimize annual average active power losses there were analyzed several connection scenarios for the renewable energy sources. The connection of wind system to bus 9 and the PV system to bus 10, leads to a value of 98,97 kW, corresponding to the optimal location of RES from all the 20 scenarios studied. The first bus represents the location of the wind power plant, and the second one the location of the photovoltaic power plant.

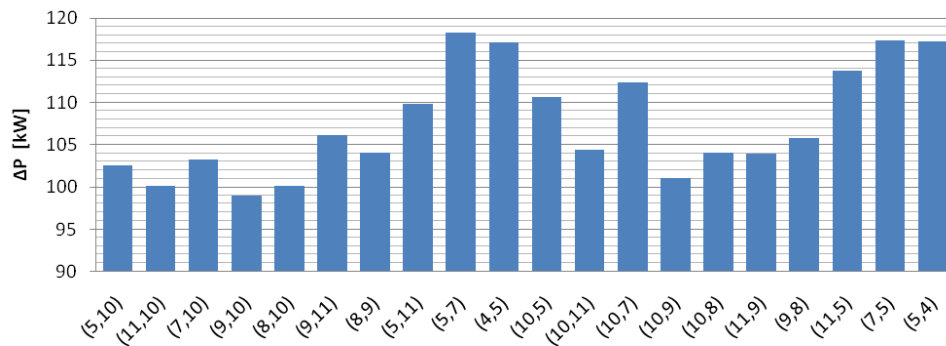


Fig. 10. Connecting RES in different buses.

4. Conclusions

In this paper, a study of the impact of renewable energy sources has on a distribution electric network has been performed. It was analyzed the main state quantities of the network elements, having known: the characteristics of underground medium voltage cables, recordings of the energy meters of load profiles along with the wind and solar powers generation.

The connection of the wind and PV system pursued the influence on the voltage magnitude, lines loading and active power losses. The presence of renewable energy sources has led to a decrease of the annual active energy losses by approximately 19%. Based on the results achieved regarding the voltage level at bus 5 and 10 where RES are connected, the maximum values reached 20,24 kV at bus 10 and 20,04 kV at bus 5. It can be noted that the most significant variation is achieved at bus 10 where voltage range between 18,99 kV and 20,24 kV.

Connecting distributed sources to the distribution electric network changes the circulation of current / power through these sections. When the generated power will cover all the loads demand, the surplus will serve to supply the nearest ones. Thus, for 10,3 % of the study time, the excess of PV and wind system power is injected to load bus 4 and 9.

REFERENCES

- [1] A. Zervos, C. Lins, U. Trenker *et.al.*, Renewable energy in Europe, Second Edition, 2010.
- [2] Carmen L.T.Borges, Djalma M. Falcao, Impact of distributed generation allocation and sizing and reliability, losses and voltage profile, IEE Bologna Power Tech Conference, 2003.
- [3] D. Parmar, L. Yao, Impact of unbalanced penetration of single phase grid connected photovoltaic generators on distribution network, UPEC Germany, 2011.
- [4] D. Patel, R.K. Varma, Impact of wind turbine generators on network resonance and harmonic distortion, IEEE, 2010.
- [5] J. Zhu, W.Gu *et. al.*, Learning Automata-Based Methodology for Optimal Allocation of Renewable Distributed Generation Considering Network Reconfiguration, IEEE, 2017.
- [6] H. Abdel-mawgoud, S. Kamel, Optimal Allocation of Renewable DG Sources in Distribution Networks Considering Load Growth, Nineteenth International Middle East Power Systems Conference (MEPCON), Menoufia University, 2017.
- [7] I. Tanaka, H. Ohmori, Scenario Generation with Clustering for Optimal Allocation of Renewable DG", IEEE Innovative Smart Grid Technologies, Asia, 2016.
- [8] Ghe. Georgescu, M. Gavrilăș, Daniela Rădășanu, Calculul și reducerea pierderilor de putere și energie în rețelele electrice (Calculation and reduction of power and energy losses in electrical networks), Editura Spectrum Iași, 1997.
- [9] A. Badea, H. Necula, Surse regenerabile de energie (Renewable energy sources), Editura Agir, 2013.
- [10] 2030 climate & energy framework, https://ec.europa.eu/clima/policies/strategies/2030_en#tab-0-0.
- [11] M. Eremia (Editor) *et al.*, Electric Power Systems, Electric Networks, Volume 1, Editura Academiei Romane, 2006
- [12] M. Eremia, H. Crișcu, B. Ungureanu, C-tin. Bulac, Analiză asistată de calculator a regimurilor sistemelor electroenergetice (Computer assisted analysis for power flow power systems), Editura Tehnică București, 1985.